SUPPLEMENTARY MATERIALS

Figures S1 to S12

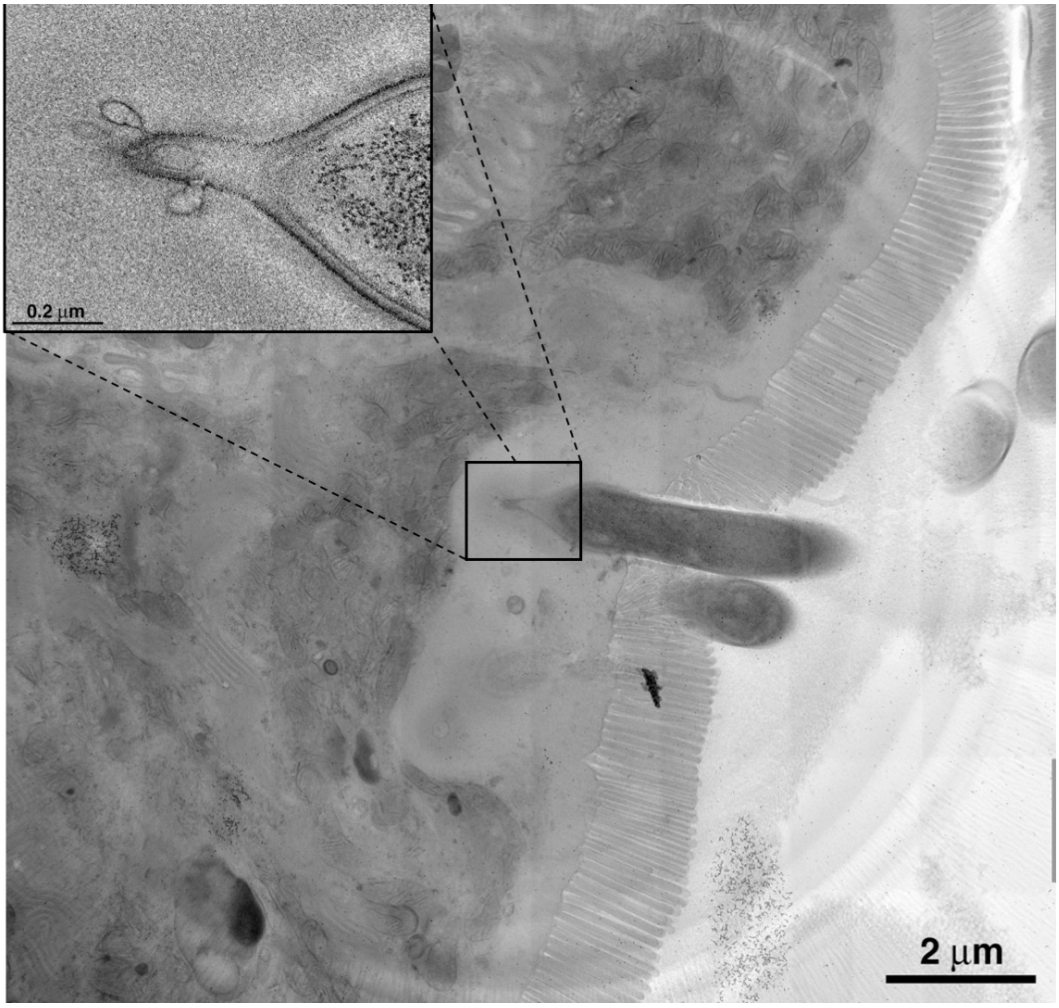

Figure S1. Formation of membrane vesicles at the distal end of the SFB-IEC synapse. Overview section and an electron tomogram (insert) of SFB interacting with an epithelial cell in the terminal ileum.

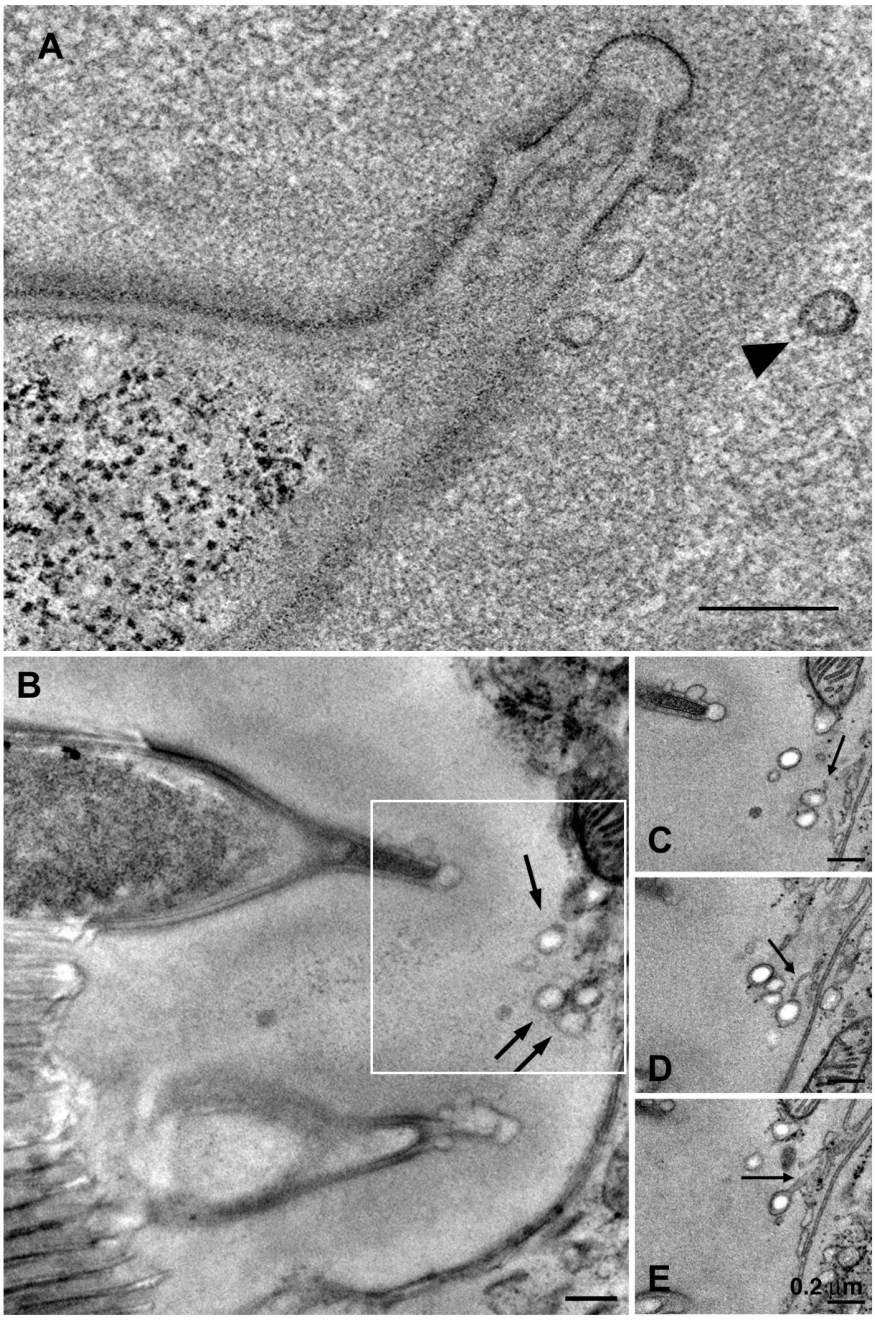

Figure S2. MATE vesicles are released into host epithelial cells. (A) Free vesicle (arrowhead) in proximity of budding MATE vesicles of an SFB-IEC synapse from terminal ileum of a C57BL/6 mouse. (B) SFB in terminal ileum of a Balb/c mouse. Several free vesicles with densities similar to budding MATE vesicles are present in the IEC cytosol around the SFB holdfast (arrows). (C-E) Higher magnification views of these vesicles show that they are connected to the IEC cytosolic tubular vesicular network (arrows).

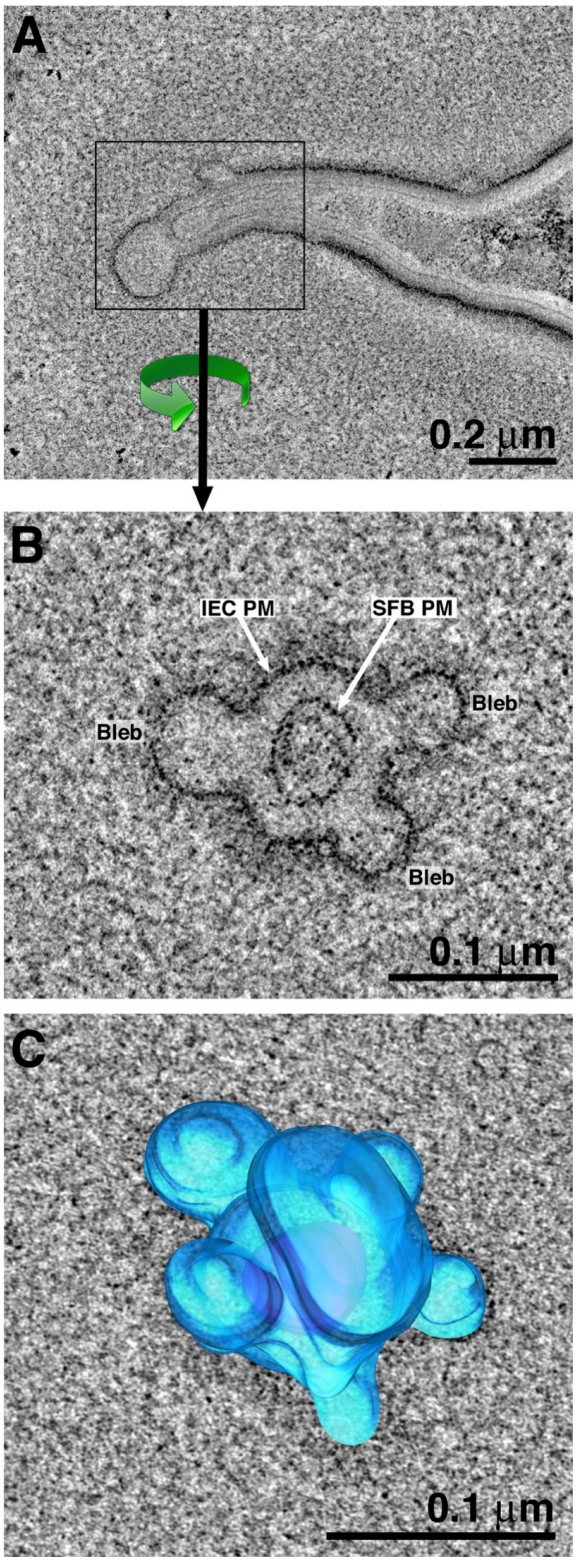

Figure S3. MATE vesicles form from the host IEC plasma membrane. Electron tomography of the distal end of an SFB-IEC synapse. (A,B) tomographic sections in longitudinal (A) and transversal (B) view. The SFB plasma membrane (PM) remains uninterrupted and the blebs originate from the IEC PM. (C) Computer-generated reconstruction of the tip of the synapse showing IEC PM in blue and the SFB holdfast in magenta.

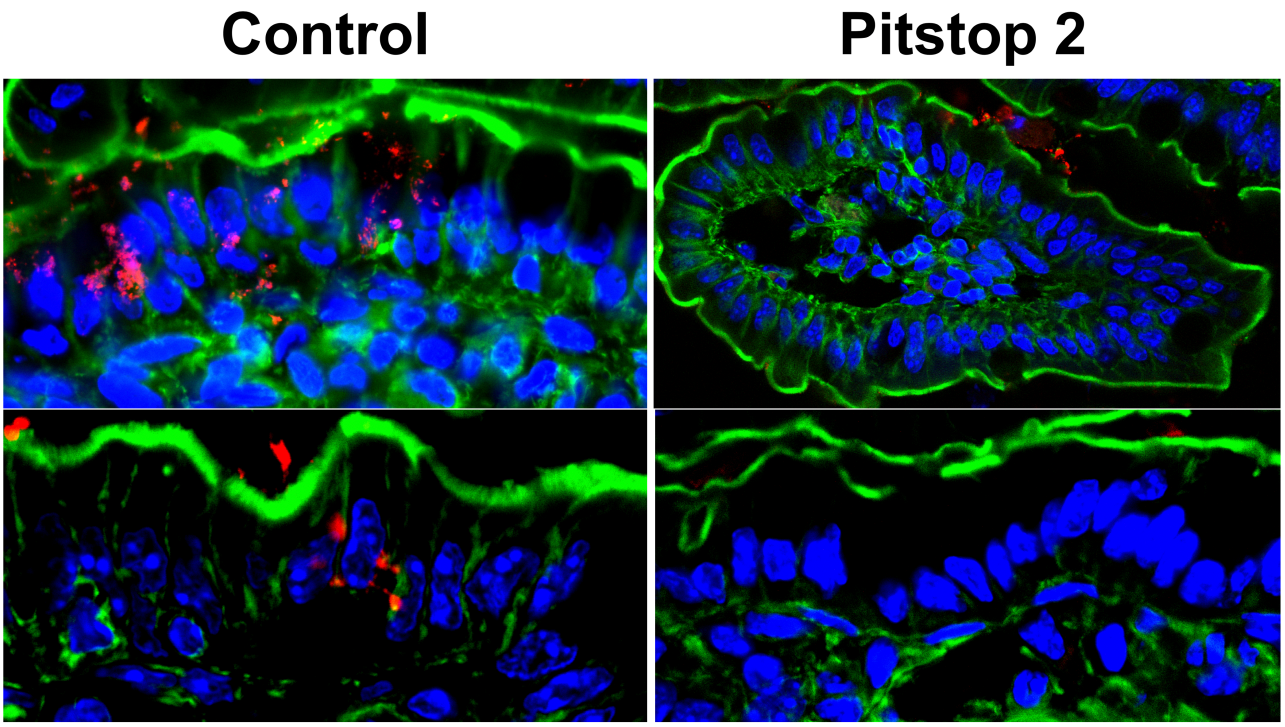

Figure S4. Pitstop 2 inhibits clathrin-dependent endocytosis of fluorescently labeled IgG. Externalized loops from terminal ileum of SFB-colonized mice were perfused with Cy3-IgG (red) in the presence or absence of Pitstop 2. Sections were co-stained with phalloidin-Alexa488 (green) and DAPI (blue) for identification of IEC borders and nuclei respectively.

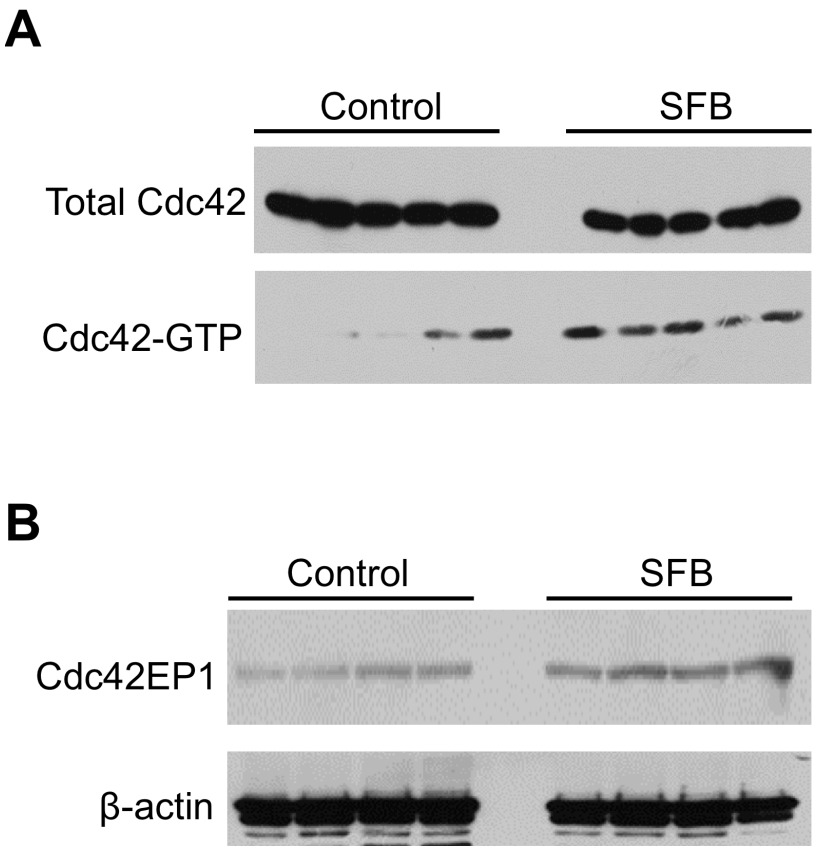

Figure S5. SFB colonization leads to CDC42 activation in IECs. SFB-negative C57BL/6J mice (Control) were colonized with SFB by oral gavage. CDC42 activation was assessed by immunoprecipitation of activated CDC42-GTP (A) and Western blot for the CDC42 adaptor protein CDC42EP1 (B) in intestinal epithelial cells (IECs) isolated from terminal ileum 10 days after SFB colonization. Lanes, represent individual animals.

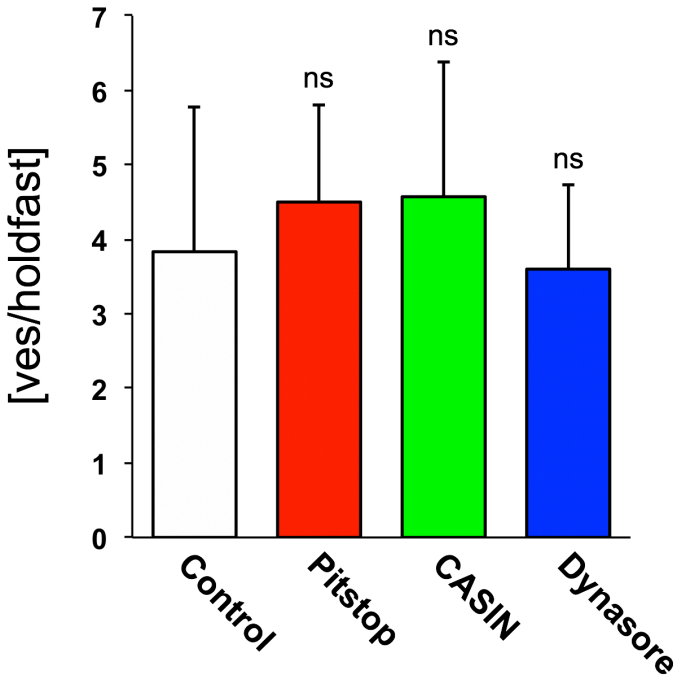

Figure S6. Endocytosis inhibitors do not affect vesicle numbers in pre-formed vesicles. SFB-colonized NSG mice were treated with the indicated inhibitors in externalized intestinal loops as described in Methods. MATE vesicles were counted from electron tomograms and results are presented as number of vesicles per bacterial holdfast.

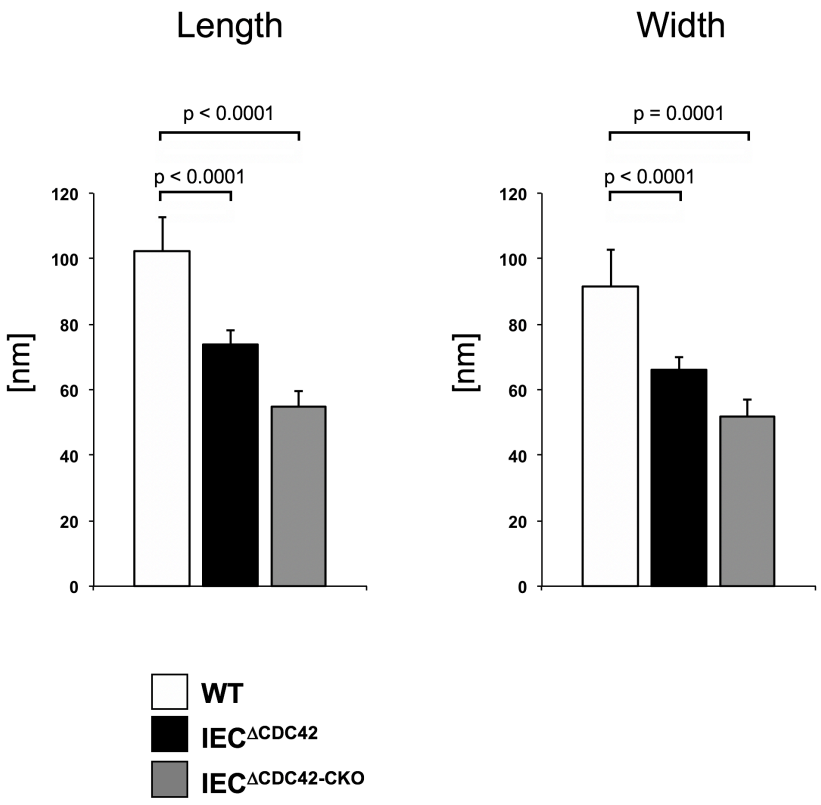

Figure S7. Disruption of normal MATE vesicle morphology in mice with conditional inactivation of CDC42 in intestinal epithelial cells. Quantification of MATE vesicle size in SFB holdfasts in the terminal ileum of $IEC^{\Delta CDC42}$, tamoxifen treated $IEC^{\Delta CDC42\text{-}CKO}$ and control B6 mice. Error bars, standard deviation. Statistics, unpaired two-tailed *t* test.

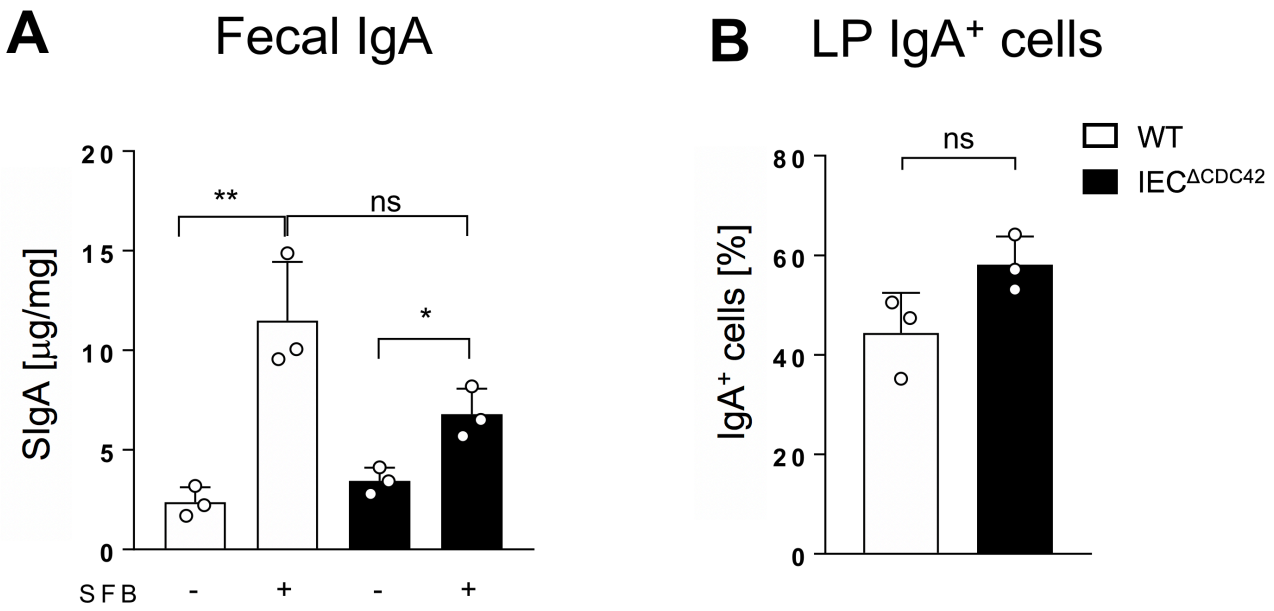

Figure S8. Normal induction of IgA responses in the absence of epithelial CDC42. SFB-negative littermate WT and IEC$^{\Delta CDC42}$ mice were colonized with SFB. (A) Secretory IgA (SIgA) in feces of WT and IEC$^{\Delta CDC42}$ mice before and 3 weeks after colonization with SFB. (B) IgA-positive plasma cells in the small intestinal lamina propria of WT and IEC$^{\Delta CDC42}$ mice 3 weeks after colonization with SFB.

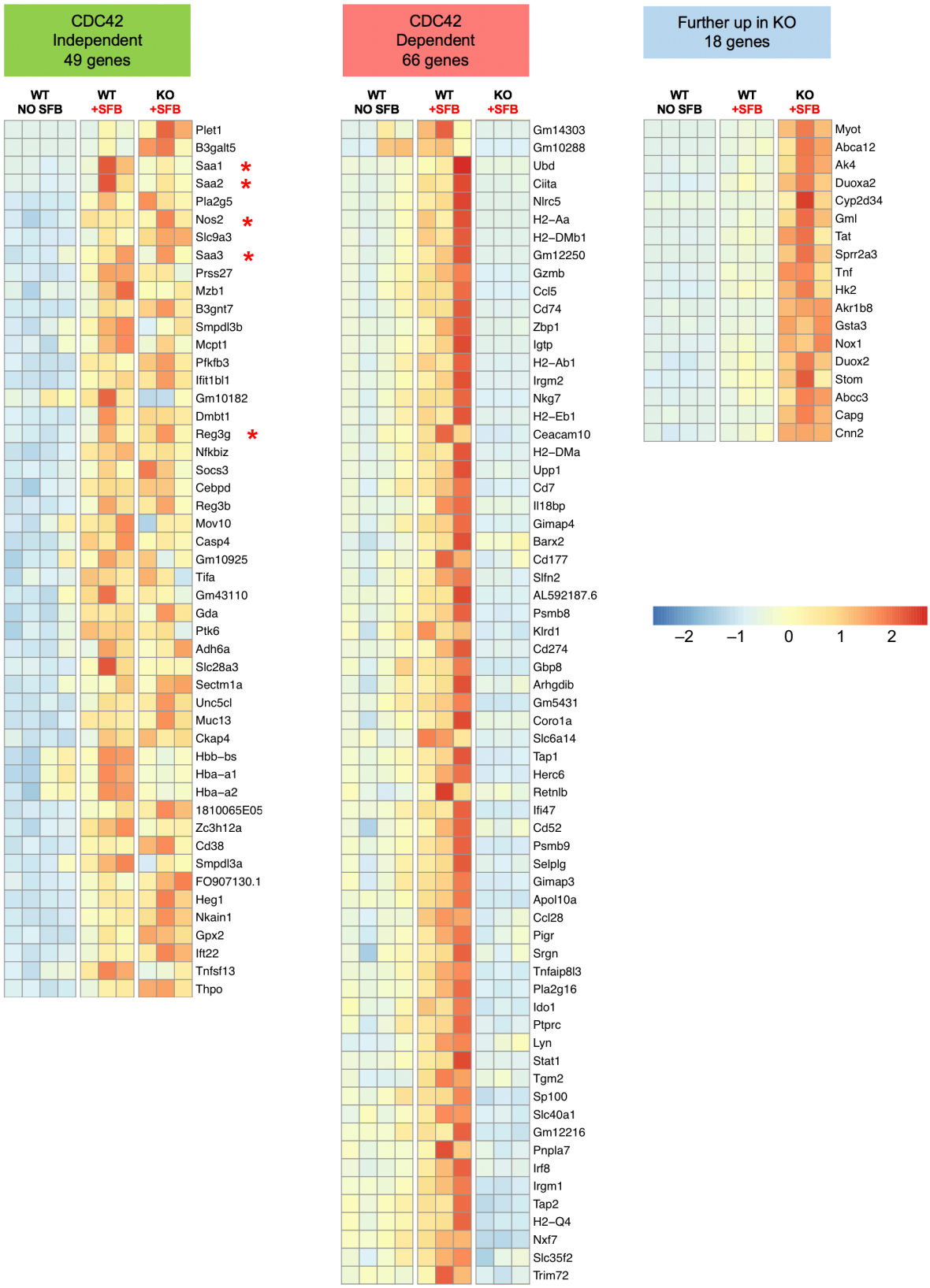

Figure S9. Differential expression of SFB-induced genes (Upregulated genes). RNA was isolated from IECs from terminal ileum of WT and IEC$^{\Delta CDC42}$ (KO) mice before and after SFB colonization (see Methods). Genes upregulated by SFB at least two fold in WT IECs were divided in three groups based on their levels in the KO+SFB group. Group 1 (CDC42-independent), genes that do not significantly change between KO+SFB and WT+SFB groups, or change less than 2 fold; Group 2 (CDC42-dependent), genes that decrease at least 2 fold in KO+SFB vs WT+SFB; Group 3 (Further up in KO), genes that increase more than 2 fold in KO+SFB compared to WT+SFB. Genes in Groups 1 and 2 are presented on Figure 7H. Red stars, genes noted on Figure 7H.

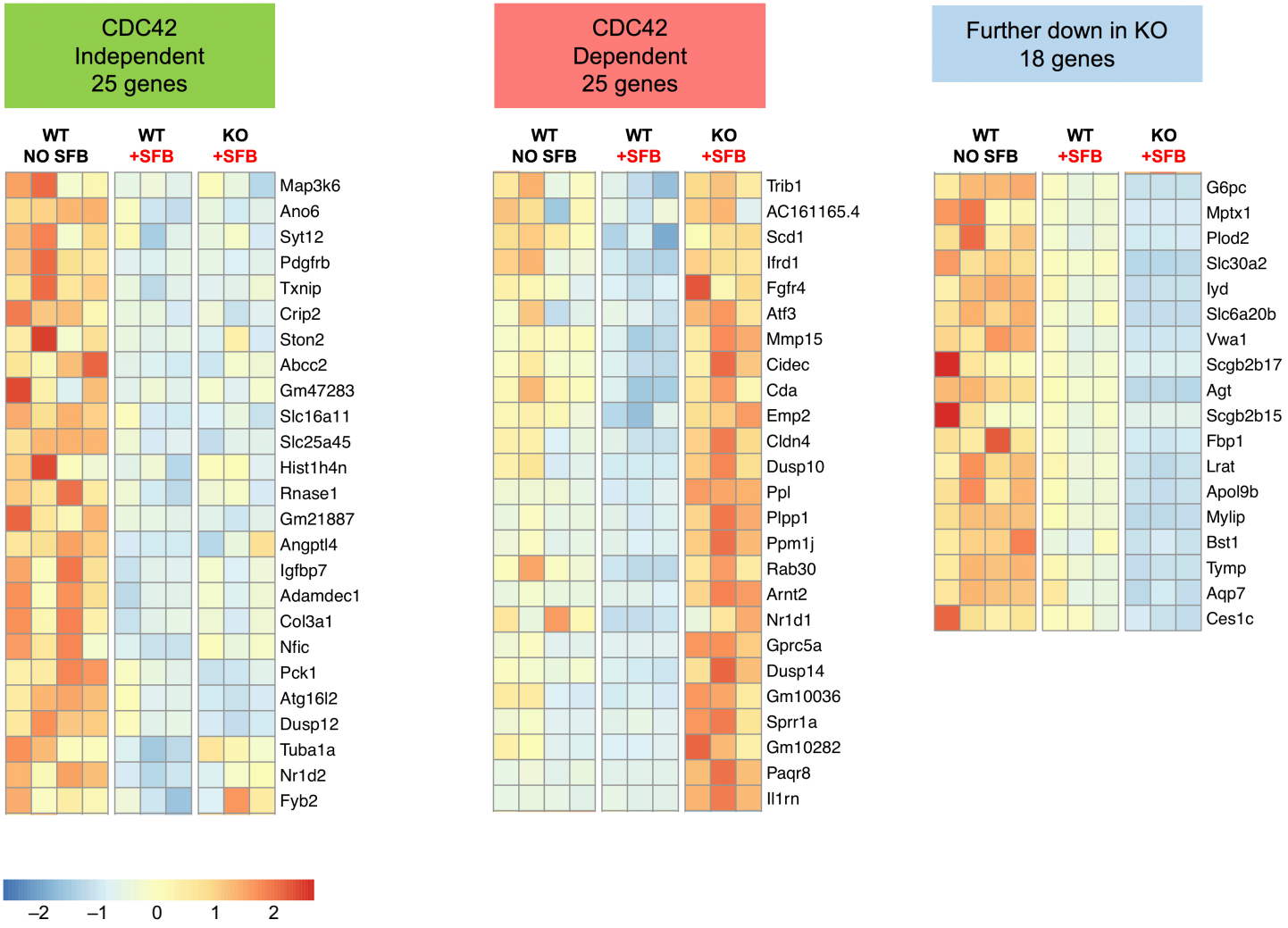

Figure S10. Differential expression of SFB-induced genes (Downregulated genes). RNA was isolated from IECs from terminal ileum of WT and IEC$^{\Delta CDC42}$ (KO) mice before and after SFB colonization (see Methods). Genes downregulated by SFB at least two fold in WT IECs were divided in three groups based on their levels in the KO+SFB group. Group 1 (CDC42-independent), genes that do not significantly change in KO or change less than 2 fold; Group 2 (CDC42-dependent), genes that increase at least 2 fold in KO; Group 3 (Further down in KO), genes that decrease more than 2 fold in KO+SFB compared to WT+SFB.

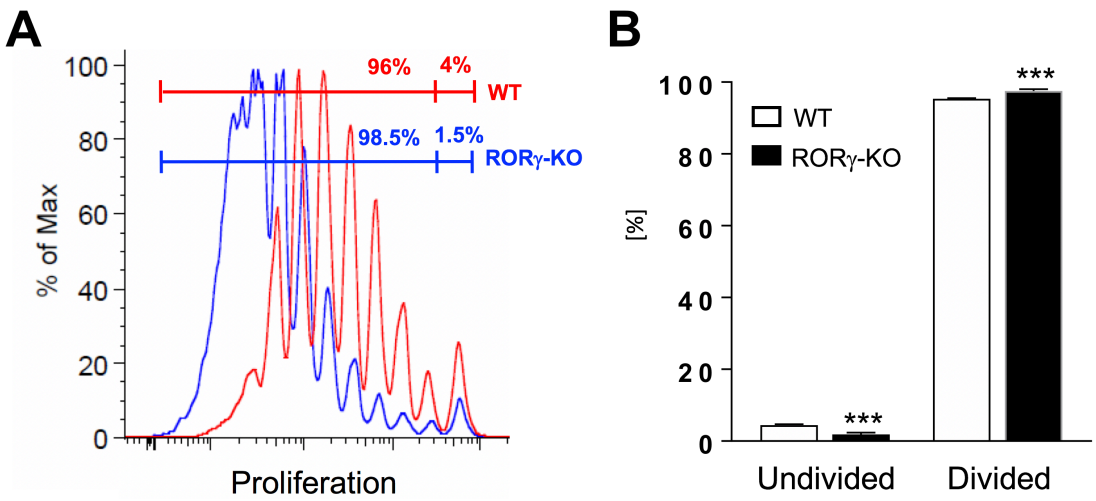

Figure S11. Activation of SFB specific T cell responses does not require antigen sampling through M cells in organized gut-associated lymphoid tissues (GALT). Proliferation of adoptively transferred SFB specific 7B8 Tg T cells in WT and organized GALT-deficient RORγ-KO mice. WT and RORγ-KO mice were colonized with SFB and two days later received 5 X 10^5 naïve CD4 T cells from 7B8 Tg mice. Proliferation dye dilution of 7B8 Tg T cells was examined 4 days later in the spleen.

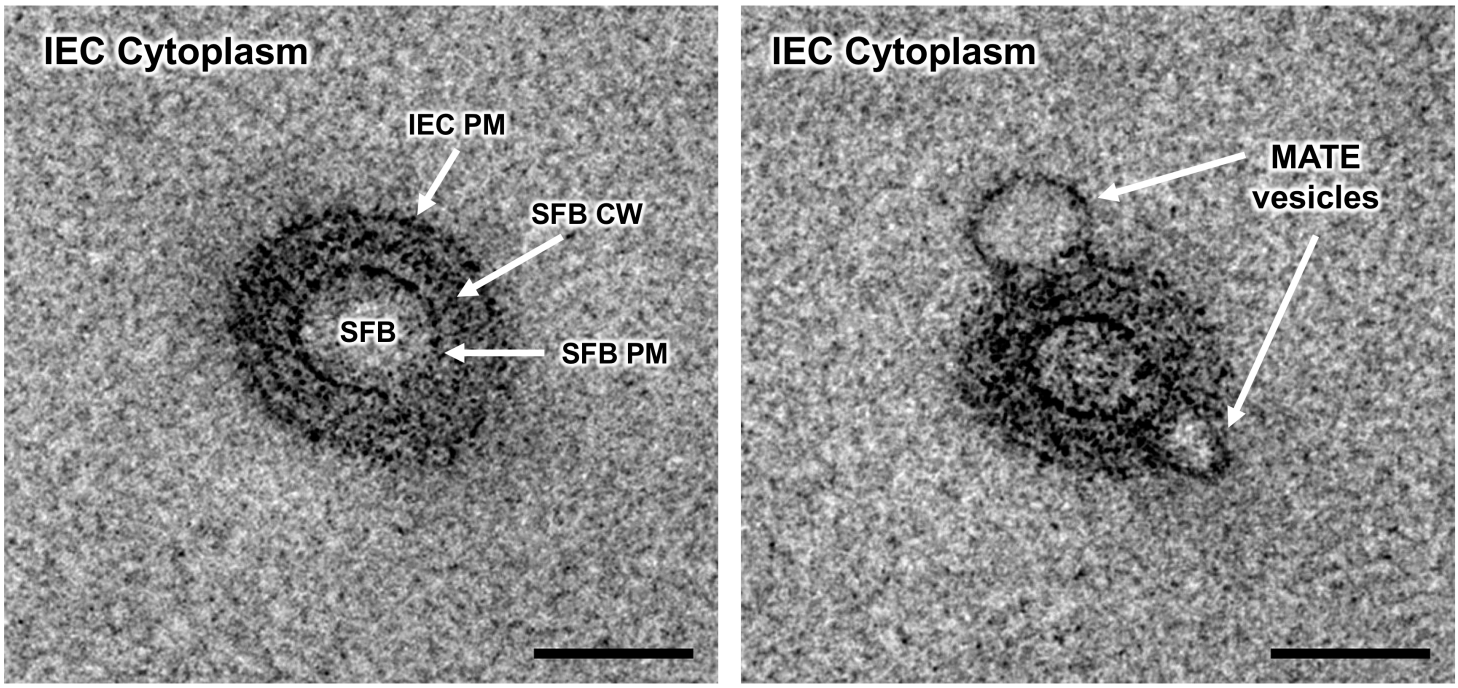

Figure S12. MATE vesicles interact with the SFB cell wall. Two consecutive sections of an electron tomogram of an SFB-IEC synapse. (Left) An SFB holdfast is seen in transversal orientation. The SFB plasma membrane (SFB PM), SFB cell wall (SFB CW), and the intestinal epithelial cell (IEC) plasma membrane (IEC PM) are evident and marked with white arrows. (Right) Section consecutive to the one on the left. The SFB plasma membrane (SFB PM) remains uninterrupted. MATE vesicles forming from the IEC PM are evident. Areas of the SFB CW are in immediate proximity and appear to associate with the open base of nascent MATE vesicles. Scale bars, 200 nm